Da Silva, SW.; Ortega Navarro, EM.; Rodrigues, M.; Bernardes, A.; Pérez-Herranz, V. (2018). The role of the anode material and water matrix in the electrochemical oxidation of norfloxacin. Chemosphere. 210:615-623. https://doi.org/10.1016/j.chemosphere.2018.07.057

Accepted Manuscript

The role of the anode material and water matrix in the electrochemical oxidation of norfloxacin

Salatiel W. da Silva, Emma M. Ortega, Marco A.S. Rodrigues, Andréa M. Bernardes, Valentín Pérez-Herranz

PII: S0045-6535(18)31315-8

DOI: 10.1016/j.chemosphere.2018.07.057

Reference: CHEM 21772

To appear in: *ECSN*

Received Date: 24 April 2018

Revised Date: 10 July 2018

Accepted Date: 11 July 2018

Please cite this article as: da Silva, S.W., Ortega, E.M., Rodrigues, M.A.S., Bernardes, André.M., Pérez-Herranz, Valentí., The role of the anode material and water matrix in the electrochemical oxidation of norfloxacin, *Chemosphere* (2018), doi: 10.1016/j.chemosphere.2018.07.057.

THE ROLE OF THE ANODE MATERIAL AND WATER MATRIX IN THE ELECTROCHEMICAL OXIDATION OF NORFLOXACIN

Salatiel W. da Silva[1,2], Emma M. Ortega[1], Marco A. S. Rodrigues[3], Andréa M. Bernardes[2], Valentín Pérez-Herranz[1*]

[1]Grupo IEC. Departamento de Ingeniería Química y Nuclear, E.T.S.I. Industriales, Universitat Politècnica de València. P.O. Box 22012, E-46071 Valencia, Spain.

[2]Departamento de Materiais, PPGE3M, Universidade Federal do Rio Grande do Sul. Avenida Bento Gonçalves, 9500, Porto Alegre, Brazil.

[3]Universidade Feevale, Campus II ERS-239, 2755, Novo Hamburgo, Brazil.

*Corresponding author: vperez@iqn.upv.es; P.O. Box 22012, E-46071 Valencia, Spain

ABSTRACT

The roles of the anode material, boron-doped diamond (BDD), with different boron (B) and substrate Silicon (Si) or Niobium (Nb) content, and one dimensionally stable anode (DSA®), were evaluated in the oxidation of norfloxacin (NOR) by electrochemical advanced oxidation process (EAOP). The effect of other components in real wastewater on the performance of EAOP was also studied. The anode materials were characterized by cyclic voltammetry, regarding diamond quality, electro-generation of oxidants and NOR oxidation mechanism (direct and/or indirect). The results showed that the anode material influences on the NOR oxidation pathway, due to distinct characteristics of the substrate and the coating. Apparently, low difference in diamond-sp^3/sp^2-carbon ratio (Si/BDD_{100} × Si/BDD_{2500}) does not leads to significant differences in the EAOP. On the other hand, the variation in the sp^3/sp^2 ratio seems to be higher when Si/BDD_{2500} and Nb/BDD_{2500} are compared, which would explain the best current efficiency result for Si substrate. However,

the Nb substrate presented a similar current efficiency and a 60% lower energy consumption. Dissolved organic matter (DOM) present in the real wastewater affect the EAOP-Nb/BDD due to $HO^{\bullet}$ and persulfate ions scavenged. However, when supporting electrolyte was added to a real wastewater spiked with NOR, the NOR decay reaches similar values found to the synthetic one. Due to the energy saving and mechanical properties, Nb substrate presents some technological advantages in relation to Si, which can facilitate the application to industrial levels.

KEYWORDS: BDD electrodes; Silicon and Niobium; Norfloxacin; Real wastewater.

1. INTRODUCTION

The widespread use and environmental prevalence of pharmaceutical compounds increase annually due to the widening range of medical treatments, greater availability and access of medicines worldwide. Pharmaceutical products reach the wastewater treatment plants (WWTP) through the wastewater network, after metabolism and excretion, as unchanged compounds or as metabolites. Besides that, direct release may occur through improper disposal of unused or expired pharmaceuticals directly into toilet bowls, sinks or as solid waste (Ternes, 1998).

Fluoroquinolones have been widely used as antibiotics in the treatment of infectious diseases (Kümmerer, 2009), as cattle growth promotor (Thiele-Bruhn, 2003) and at aquaculture (van den Bogaard and Stobberingh, 1999). Considering the overall use and the partial or complete resistance of most fluoroquinolones to the elimination in conventional WWTP, they are often detected in effluents, surface water and drinking water (Miao et al., 2004). Moreover, the fluoroquinolones Ciprofloxacin, Enrofloxacin, Danofloxacin and Norfloxacin were found in soil samples from São Paulo (Leal et al., 2013). *Streptococcus agalactiae* have also been reported to be resistant to fluoroquinolone antibiotics in fish farms in Brazil (Chideroli et al., 2017). Therefore, the

removal of these antibiotic class before the discharge to the environment is a technological challenge.

Advanced oxidation processes (AOP) have been employed in the removal of pharmaceutical compounds, including Fenton, UV_{254nm} and H_2O_2/UV_{254nm} (Santos et al., 2015), Photocatalysis and Photoelectrocatalysis (da Silva et al., 2018), among other combinations. The electrochemical advanced oxidation process (EAOP) has been highlighted among the AOP to contaminants removal (Isarain-Chávez et al., 2017; Souza et al., 2017) due to its ease implementation, operation and scale-up and low energy consumption (de Moura et al., 2014).

The degradation of different organic compounds by EAOP at boron-doped diamond on Silicon substrate (Si/BDD) has been extensively reported (de Araújo et al., 2014; Barreto et al., 2015; Brito et al., 2015; Coledam et al., 2016; Souza et al., 2017). However, the electrochemical degradation in BDD on Niobium substrate (Nb/BDD) has been poor studied. The applicability of Nb/BDD anodes in the oxidation of organic compounds has been successfully used to remove carboxylic acids (de Queiroz et al., 2017), dyes (Sales Solano et al., 2013), petroleum (Gargouri et al., 2014) and agricultural pesticides (Borràs et al., 2010). Nevertheless, no studies have been reported about electrochemical oxidation of norfloxacin (NOR) in Nb/BDD anodes.

The main goal of this work was to evaluate the degradation of NOR by EAOP. The influence of the anode material and the role of other components in real wastewater on the EAOP performance were evaluated. The different anode materials were characterized by cyclic voltammetry, regarding to the electrochemical window, oxygen evolution reaction (OER), diamond film quality (diamond-sp^3/sp^2-carbon ratio), electro-generation of oxidants and evaluation of the NOR oxidation mechanism (direct and/or indirect). Besides that, the prediction of NOR decay was proposed by using a mathematical model. The role of other components in real wastewater was approached by the evaluation of NOR oxidation in deionized water and in a real domestic wastewater.

2. EXPERIMENTAL

2.1 Chemicals and solutions

Norfloxacin active compound was purchased in a local pharmacy (≥ 98%), anhydrous sodium sulfate and all chemicals for chemical oxygen demand (COD) analysis were purchased from Panreac (≥ 99%). NaOH, Na_2CO_3, $NaHCO_3$ and H_2SO_4 were of analytical grade supplied by Merck. Ultrapure water (Millipore Milli-Q system, resistivity ≥18.2 MΩ cm) was used for standard solutions preparation. Deionized water (conductivity 1 μS cm^{-1}) was used for the preparation of all work solutions.

A real wastewater (RWW) was collected after the secondary treatment by activated sludge in the municipal domestic wastewater treatment plant from Novo Hamburgo/Brazil in November 2017. Thereafter, the real wastewater was characterized by UV-Vis spectroscopy, COD, Ion chromatography (IC) and pH and the results are summarized in Fig. SM-1 and table SM-1 in supplementary material (SM).

Before the treatment by EAOP, the real wastewater was spiked with 0.1 mM NOR to attain comprehensive NOR decay profiles (NORE). The conductivity value of the NORE was 5 times lower than the one found for the solution commonly used as background electrolyte in EAOP (0.05 M Na_2SO_4) (Brillas et al., 2009). For these considerations, one assay was performed without the addition of the supporting electrolyte (NORE), and another one was accomplished with the addition of 0.01 M Na_2SO_4 in the real wastewater spiked with 0.1 mM NOR (NORES). To compare the results with those obtained for synthetic solution (NOR), the initial pH of NORE and NORES was adjusted to ~4.

The RWW has no absorbance shoulder at the wavelength 240-400 nm. Nevertheless, when the target contaminant was spiked in the wastewater matrix, the characteristic NOR peak appear, and this characteristic not changes when the supporting electrolyte was also added (Fig. SM-1a).

2.2 Electrochemical measurements

The electrochemical measurements were performed using a conventional three electrode cell connected to a computer-controlled Autolab potentiostat/galvanostat model PGCTAT 302N at a scan rate of 100 mV s^{-1}. The cell used Ag/AgCl (3 M KCl) as reference electrode and platinum (Pt) as counter electrode. The working electrodes used were a dimensionally stable anode (DSA®) and BDD anodes: Si/BDD with distinct boron content [B] = 100 and 2500 ppm and Nb/BDD with [B] = 2500 ppm. At this work, the boron content was expressed in ppm regarding to mg kg^{-1}. The main characteristics of these electrodes are summarized in supplementary material at table SM-2.

2.3 Electrochemical oxidation

All oxidation assays of the NOR antibiotic were performed on a single compartment filter-press flow cell by using flat square electrodes with a geometric surface area (A_s) of 0.01 m^2. 1 L of the electrolyte solution was stored in a double-jacket reservoir and circulated through the cell by a centrifugal pump with a flow rate (Q) of 8.33 × 10^{-6} m^3 s^{-1}, that delivery a mass transport coefficient (k) of 2.30 × 10^{-6} m s^{-1} estimate by the $(Fe(CN)_6^{4-})/(Fe(CN)_6^{3-})$ system (Cañizares et al., 2006). The electrochemical oxidation process was performed in galvanostatic mode. During the EAOP the pH was continuously monitored but no pH control was performed. The scheme of the EAOP is presented on the supplementary material (Fig. SM-2).

The anodes were tested to evaluate the effect of boron content and diamond-sp^3/sp^2-carbon ratio (Si/BDD_{100} and Si/BDD_{2500}); the influence of the diamond film substrate Silicon or Niobium (Si/BDD_{2500} and Nb/BDD_{2500}); the effect of the anode non-active vs. active for OER (Nb/BDD_{2500} and DSA®); and the role of other components in real wastewater on the performance of EAOP (Nb/BDD_{2500}).

124

125 **2.4 Analyses**

126 Changes in the UV/Vis absorption spectrum of the NOR were evaluated by UV/Vis
127 spectroscopy (T80 + UV/Vis Spectrometer from PG Instruments Ltd) using quartz cuvettes with a
128 10 mm optical path. Spectra were obtained between wavelengths 190-900 nm.

129 Based on the absorption band at 272 nm, which was previously confirmed by UV/Vis
130 (supplementary material, Fig. SM-1), a concentration vs. absorbance curve was constructed and
131 NOR decay could be monitored. Therefore, NOR conversion (X_{NOR}, %) was calculated using Eq. (1):

132 $$X_{NOR}(\%) = (C_0 - C)/C_0 \times 100 \quad (1)$$

133 where C_0 is the NOR concentration at initial time and C is the NOR concentration at n time.

134 The COD in mg of O^2 L^{-1} was evaluated using the closed reflux colorimetric method
135 according to the Standard Methods (Rice et al., 2017) and the COD conversion (X_{NOR}, %) was
136 calculated by the Eq. (2).

137 $$X_{COD}(\%) = (COD_0 - COD)/COD_0 \times 100 \quad (2)$$

138 where COD_0 is the COD concentration at initial time and COD is the COD concentration at n time.

139 To better evaluate the results obtained, some discussions will be based on current
140 efficiency (Eq. (3)) and energy consumption (Eq. (4)) calculated from COD values (García-Galbadón
141 et al., 2006).

142 $$\phi = F \cdot V_L \cdot (COD_0 - COD)/8 \cdot \int_0^t I(t)dt \quad (3)$$

143 $$E_s = \int_0^t U(t) \cdot I(t)dt/6000 \cdot V_L \cdot (COD_0 - COD) \quad (4)$$

144 where F is the Faraday constant (96500 A s^{-1} mol^{-1}), I is the applied current (A), V_L is the
145 electrolytic solution (L), t is the time in second (s) and U is the cell voltage (V).

146 The pH was monitored by potentiometric method by using micropH 2000 Crison.

The IC was performed in DIONEX ICS 3000 coupled to a conductivity detector. For the anions and cations, the column used was IonPac® AS23 2 mm × 250 mm and the IonPac® CS12A 2 mm × 250 mm, respectively. The mobile phase consists in 4.5 mM Na_2CO_3 and 0.8 mM $NaHCO_3$ for the anion detection and 11 mM H_2SO_4 for the cations identification.

3. RESULTS AND DISCUSSION

3.1 Electrochemical measurements

3.1.1 Electrodes characterization

According to the literature (Watanabe et al., 2010; Einaga et al., 2014), it is possible to evaluate the quality of diamond films in BDD electrodes by cyclic voltammetry in a background solution containing 0.5 M H_2SO_4 (supplementary material, Fig. SM-3). It was observed in Fig. 1a and 1b that the used BDD electrodes have a low background current and high potential for OER, meaning that these electrodes have a high diamond-sp^3 content with low carbon-sp^2 impurities at the surface of the diamond films. The obtained voltammogram are in agreement with those finding in the literature (supplementary material, Fig. SM-3, shape II) (Watanabe et al., 2010).

Fig. 1a also demonstrated that the background current rises and the working potential window changes to less positive potentials as the level of boron doping increases, due to the increase in the carbon-sp^2 impurities (Martin et al., 1996). In addition, the substrate Si or Nb for the BDD film also affect the sp^3/sp^2 ratio, and for this case, Nb appears to have higher carbon-sp^2 impurities than the Si substrate for BDD (Fig. 1b).

A raised background current for DSA® electrode which has high adsorption capacity and low potential for oxygen evolution (~1.25 V vs. Ag/AgCl) (Panizza and Cerisola, 2009) was exhibited in the voltammogram (Fig. 1c). These results also show a reversible anodic shoulder in ~0.7 V vs. Ag/AgCl which corresponds to the solid state redox transitions $RuO_2 \leftrightarrows Ru_2O_3$ (Galizzioli et al., 1974; Pelegrini et al., 1999).

Based on the voltammogram it is verified that it possible electro-generate more $HO^{\bullet}$ with less parasitic reactions in the electrode materials: Si/BDD_{100} > Si/BDD_{2500} > Nb/BDD_{2500} > DSA®.

FIG. 1

3.1.2 Electrochemically generation of oxidants

Garcia-Segura et al. (2015) state that the alterity in diamond-sp^3/sp^2-carbon ratio promotes substantial variations in the electrochemical generation of oxidants from supporting electrolyte. In this way, the electrocatalytic property of the anode materials for generation of oxidants were evaluated by cyclic voltammetry in 0.1 M Na_2SO_4.

An anodic shoulder (I) in the potential region of ~2 V vs. Ag/AgCl corresponding to the oxidation of the electrolyte support, generating the persulfate ion ($S_2O_8^{2-}$), and a cathodic shoulder (II) linked to reduction of the persulfate ion (Serrano et al., 2002; Provent et al., 2004), were found for Fig. 2a, 2b and 2c.

Studies have demonstrated that there are two possibilities for the generation of persulfate ions (Serrano et al., 2002; Davis et al., 2014; Barreto et al., 2015). In the first case, the HSO_4^- and / or SO_4^{2-} anions can adsorb at the active sites formed by carbon-sp^2 impurities to form $SO_4^{\bullet-}$ (Davis et al., 2014) that leads to $S_2O_8^{2-}$ generation. The other one occurs by the indirect oxidation of ions HSO_4^- and SO_4^- by $HO^{\bullet}$ electrogenerated on the anode surface, following the steps presented in Eq. (5-8) (Serrano et al., 2002).

$$BDD + H_2O \rightarrow BDD(HO^{\bullet}) + H^+ + e^- \quad (5)$$

$$HSO_4^- + HO^{\bullet} \rightarrow SO_4^{\bullet-} + H_2O \quad (6)$$

$$H_2SO_4 + HO^{\bullet} \rightarrow SO_4^{\bullet-} + H_3O^+ \quad (7)$$

$$2\,SO_4^{\bullet-} \rightarrow S_2O_8^{2-} \quad (8)$$

It is still possible to verify an increase in the electrochemical generation of persulfate ions as the boron concentration increases (Fig. 2a and 2b). This fact was more apparent for Nb/BDD_{2500}

electrode (Fig. 2c). This increase in the production of $S_2O_8^{2-}$ can be linked to the retention of sulfate species in carbon-sp² impurities that have higher adsorption properties than diamond-sp³ (Davis et al., 2014; Barreto et al., 2015) favoring the persulfate ion generation. In fact, the electro-generation of persulfate ions will be more pronounced in the Nb/BDD_{2500} then Si/BDD_{2500} and Si/BDD_{100}.

The persulfate ions are also generated on the surface of the DSA® electrode, following Eq. (6-8) or through the interaction of the transition metal catalyst (RuO_2) present in the DSA® electrode (Panizza and Cerisola, 2009; Isarain-Chávez et al., 2017) (Fig. 2d). Therefore, it is necessary to consider that the oxidation of NOR will not be exclusively mediated by hydroxyl radicals, but also by persulfate ions.

FIG. 2

3.1.3 Electrochemical behavior of norfloxacin

Aiming to elucidate if direct oxidation of NOR occurs, cyclic voltammetry assays were performed on BDD and DSA® electrodes, adding a 1.25 M NOR in a background solution containing 0.1 M Na_2SO_4.

For Si/BDD_{100}, by adding a known concentration of NOR an anodic perturbation was found, which may be related to the direct oxidation of NOR (Fig. 3a). On the other hand, it is possible to identify for Si/BDD_{2500} and Nb/BDD_{2500}, a well-defined anodic oxidation shoulder at ~1,3 V vs. Ag/AgCl (Fig. 3b and 3c). This means that the antibiotic NOR can interact with the surface of these electrodes, resulting in a direct transfer of electrons (direct oxidation). Likewise, for the Si/BDD_{2500} and Nb/BDD_{2500} (Fig. 3b and 3c) it is also possible to see an anodic perturbation at ~ 1.7 V vs. Ag/AgCl that can be related to the direct oxidation of an intermediate product from NOR oxidation (Coledam et al., 2016).

The difference found for direct oxidation of NOR can be related to its content of carbon-sp^2 impurities in BDD films shown in Fig. 1. For higher carbon-sp^2 contents (Nb/BDD_{2500} > Si/BDD_{2500} > Si/BDD_{100}), higher adsorption of NOR at the electrode surface is expected, therefore, the detection of anodic shoulders is better-defined.

The voltammogram for DSA® not shows an anodic and/or cathodic shoulder related to direct NOR oxidation, indicating that this pollutant will be oxidize only by hydroxyl radicals, persulfate ions and the transitions of RuO_2. Similar results for other pollutants and electrodes of the DSA® type have already been reported in the literature (Heberle et al., 2017).

FIG. 3

3.2 Effect of boron content and diamond-sp^3/sp^2-carbon ratio

It is known that an increasing in the boron concentration in the growing diamond film increases the carbon-sp^2 impure phases (Einaga et al., 2014). These carbon-sp^2 affects the OER (generation of $HO^{\bullet}$), the electro-generation of oxidants through the supporting electrolyte and NOR interaction with BDD surface (direct oxidation), which can be confirmed in Fig. 1, 2 and 3, respectively. In this sense, the boron concentration and the diamond-sp^3/sp^2-carbon ration were evaluated for NOR oxidation by using the Si/BDD_{100} and Si/BDD_{2500} material.

It is possible to observe in Fig. 4c and 4d that no significant differences in the current efficiency and energy consumption values, calculated for both Si/BDD_{100} and Si/BDD_{2500} anode, were observed, meaning that similar results for COD and NOR decay were achieved, Fig. 4a and 4b, respectively.

Although the results presented on Fig. 1a, 2a, 2b, 3a and 3b showed that these materials present some differences in the sp^3/sp^2 ratio, this difference did not lead to significant changes in NOR oxidation. This finding is probably associated to the small difference in the sp^3/sp^2 ratio between the anodes, what agrees with literature (de Araújo et al., 2014).

By using BDD anodes with different boron concentrations, and low differences in the sp^3/sp^2 ratio (estimated by Raman spectrometry), Fierro et al. (2011) did also not observed significant differences in the COD removal. de Araújo et al. 2014 investigated the influence of the sp^3/sp^2 ratio (165 and 176, estimated by Raman spectrometry) on Si/BDD with the same boron concentration (500 ppm) to removal of color, COD and TOC from rhodamine B, and did not verified a significant removal difference.

The findings presented at this work and corroborated by the literature (de Araújo et al., 2014) show that the difference in the diamond-sp^3/sp^2-carbon ratio probably should be higher (such as 165 and 262, as verified by de Araújo et al. 2014) to affect the contaminant oxidation.

FIG. 4

3.3 Effect of diamond film substrate (Si or Nb)

The substrate effect, silicon or niobium, of diamond film were investigated for NOR oxidation by using the Si/BDD_{2500} and Nb/BDD_{2500} anodes. Fig. 5a and 5b showed similar results in NOR degradation and COD removal for Si or Nb substrate. However, Fig. 5c shows that there is a slight difference in current efficiency for NOR oxidation using Si and Nb substrates. The differences can be attributed to the existence of competing parasitic reactions such as OER at the anode which will be more expected on the Nb/BDD_{2500}. Since this electrode presented a higher sp^2-content than Si/BDD_{2500} as show on Fig. 1b and already discussed.

Besides that, the NOR oxidation mechanism for Nb/BDD_{2500} anode may differ from Si/BDD_{2500} due to differences in the carbon-sp^2 impurities, which leads to higher direct oxidation and by persulfate ions and less by $HO^{\bullet}$ (Guinea et al., 2009; Souza et al., 2016) for Nb/BDD_{2500}.

On the other hand, the Nb/BDD_{2500} anode showed 60% less energetic consumption when compared to Si/BDD_{2500} (Fig. 5d). These can be explained by the fact that Si/BDD electrodes have

lower electrical conductivity than Nb/BDD (Chen, 2004), which was evidenced in the voltammogram (Fig. 1b). This finding could be a technological advantage over silicon, for scale-up the EAOP to industrial application.

FIG. 5

3.4 Influence of the anode material

The influence of the anode material on NOR oxidation was also investigated by using one material non-active (Nb/BDD_{2500}) and one active (DSA®) for the OER. It is possible to observe in Fig. 6a, 6b and 6c that the active electrode for the OER, the DSA®, presented a lower NOR and COD decay, as a directly consequence, a lower current efficiency for NOR oxidation was found. The oxidation power of the anode is directly related to the potential for OER. Therefore, the results obtained, for the evaluated anode DSA®, can be explained by the general oxidation mechanism for organic pollutants (Comninellis, 1994) and confirmed in the voltammetry measurements in Fig. 1c, 2d and 3d.

The nature of DSA® material causes difficulties in the NOR oxidation by $HO^{\bullet}$ due to the competition with parasitic reactions, favoring to indirect NOR oxidation through the formation/decomposition of the higher valence oxide $RuO_2 \leftrightarrows Ru_2O_3$ (Galizzioli et al., 1974; Pelegrini et al., 1999) and/or by the generation of persulfate ions (Panizza and Cerisola, 2009), significantly reducing the oxidation rate of NOR.

On the other hand, the non-active electrode for the OER, the Nb/BDD_{2500}, showed a higher NOR degradation and COD decay, as well a higher current efficiency for NOR oxidation when compared to DSA® (Fig. 6a, 6b and 6c). These result can be explained because the Nb/BDD_{2500} have a higher potential for OER ~2,30 V vs. Ag/AgCl and the $HO^{\bullet}$ is so weakly bonded to the surface of the BDD (low bonding enthalpy) that it is possible to say that the $HO^{\bullet}$ are quasi-free (Comninellis and Chen, 2010). It means that the current applied leads to a less undesired side-

296 reactions (OER) and high $HO^{\bullet}$ generation that could interact with NOR causing a high oxidation.
297 Consequently, a decrease of the electric energy consumption was exhibited for Nb/BDD_{2500} when
298 compared to DSA® (Fig. 6d).

299 **FIG. 6**

300

301 **3.5 The role of other components in real wastewater on the EAOP performance**

302 It is possible to see in Fig. 7a that NOR decay (synthetic solution) was faster than the one
303 composed by NORE (RRW spiked with NOR). These results can be explained because NOR content
304 corresponded to ~50% of COD, indicating that some COD fraction corresponded to dissolved
305 organic matter (DOM) (González et al., 2013). Thereby, DOM can affect negatively the NOR
306 degradation, since it can be involved in mechanisms of oxidant agents consumption (like $HO^{\bullet}$ and
307 persulfate ions) (Wenk et al., 2011).

308 On the other hand, when sodium sulfate was added to a NORES, the NOR degradation
309 significantly increase, reaching similar values found to degradation of synthetic solution. These
310 facts can be linked to the energy-band theory. For the solution with low conductivity (NORE), the
311 voltage may not provide sufficient potential to activate electron transfer (Lin et al., 2012) and thus
312 reduces the $HO^{\bullet}$ and persulfate ions formation. Nevertheless, the addition of the sodium sulfate
313 leads to an increase in the ionic force and conductivity of the NORES solution, favoring the
314 movement and transport of generated persulfate ions, from the surface of the anode to the bulk
315 of the solution, leading to an increased in NOR decay (Zhong et al., 2013).

316 Similar results were also found for COD decay (Fig. 7b). However, COD and NOR decay was
317 not simultaneous leading to byproduct formation. More information about of the physicochemical
318 characteristics of the wastewater treated by EAOs is showed in table SM-1 on supplementary
319 material.

Fig. 7a also shows that the NOR decay follows an exponential-like decay. Probably NOR have a low concentration when compared to an excess of $HO^{\bullet}$ generated at high current densities, which may describe the reactions as first-order kinetic (Fukunaga et al., 2008). Linearizing the results of Fig. 7a by plotting $\ln(C/C_0)$ vs. treatment time (h), the slope in the linearized plot (inset graphic in Fig. 7a will determines the kinetic constant value for NOR removal resulting in 0.75 h^{-1} (▲ NOR), 0.82 h^{-1} (● NORES) and 0.45 h^{-1} (■ NORE), respectively, with a good linear correlation $R^2 \geq 0.99$.

FIG. 7

The ion chromatography showed the presence of nitrate as an oxidation product of NOR. Therefore, the total oxidation of NOR involves the stoichiometric reaction (9).

$$C_{16}H_{18}FN_3O_3 + 38\,H_2O \rightarrow 16\,CO_2 + 3\,NO_3^- + F^- + 94\,H^+ + 90\,e^- \quad (9)$$

Based on the number of the electrons exchanged for the complete total oxidation of NOR (90), the mass transport coefficient (k, 2.30×10^{-6} m s^{-1}) and the NOR concentration at the initial treatment time (C_0, 0.1 mol m^{-3}) the limiting current density (i_{lim}) for the system was found to be 2 A m^2 (Eq. (10)) (Kapałka et al., 2008):

$$i_{lim} = n \cdot F \cdot k \cdot C_0 \quad (10)$$

Considering that the applied current density in the process was 100 A m^2, it is concluded that $I > i_{lim(0)}$, and the system is being controlled by mass transport. From the mathematical point of view, this behavior can be modeled through Eq. (11).

$$C = C_0 \cdot exp\{-t/\tau\,(1 - exp(k \cdot A_s/Q))\} \quad (11)$$

where, τ is the residence time (12 s).

The mathematical model used (simple) is generally applied to direct oxidation systems and / or in which hydroxyl radicals are the main oxidant mediators (Comninellis and Chen, 2010), which may explain the good correlation found for NOR and NORES decay. On the other hand,

differences between the degradation of organic contaminants achieved experimentally and the prediction by simple models such as the one used here have been reported (Coledam et al., 2016), and this fact was also found for NORE. These differences can be explained by the fact that, these mathematical model does not predict the possibility of electrochemically generating other oxidants (such as persulfate, hypochlorite, chlorine etc.), that can act in the bulk solution. Additionally, the model also not takes into account the generated radicals scavenger by DOM (Comninellis and Chen, 2010; Wenk et al., 2011).

4. CONCLUSIONS

The results presented at this work showed that EAOP is a good technology option for the oxidation of NOR in synthetic solutions and real wastewater. The electrode material may affect significantly the NOR and COD decay rates. A higher sp^2-content will have an influence on the NOR oxidation mechanism, favoring the direct oxidation and the one mediated by persulfate ions. On the other side, a high-quality diamond film, with high sp^3-content, will favor the oxidation by $HO^{\bullet}$ and will increase the process current efficiency. Comparing the electrodes evaluated at this work, the BDD presented the best results in terms of NOR and COD decay. In fact, considering its mechanical and conductive properties that save energy consumption, Niobium presents some technological advantages in relation to Silicon, which can facilitate the scale-up of the EAOP to industrial levels.

ACKLOWGEMENTS

The authors thanks CNPq, CAPES, Cyted, FAPERGS and Finep for the financial support.

5. REFERENCES

Barreto, J.P. P., Araújo, K.C. F., de Araújo, D.M., Martínez-Huitle, C.A., 2015. Effect of sp3/sp2 Ratio on Boron Doped Diamond Films for Producing Persulfate. ECS Electrochem. Lett. 4, E9–E11.

Borràs, N., Oliver, R., Arias, C., Brillas, E., 2010. Degradation of Atrazine by Electrochemical Advanced Oxidation Processes Using a Boron-Doped Diamond Anode. J. Phys. Chem. A 114, 6613–6621.

Brillas, E., Sirés, I., Oturan, M.A., 2009. Electro-Fenton Process and Related Electrochemical Technologies Based on Fenton's Reaction Chemistry. Chem. Rev. 109, 6570–6631.

Brito, C.D.N., de Araújo, D.M., Martínez-Huitle, C.A., Rodrigo, M.A., 2015. Understanding active chlorine species production using boron doped diamond films with lower and higher sp3/sp2 ratio. Electrochem. commun. 55, 34–38.

Cañizares, P., García-Gómez, J., Fernández de Marcos, I., Rodrigo, M.A., Lobato, J., 2006. Measurement of Mass-Transfer Coefficients by an Electrochemical Technique. J. Chem. Educ. 83, 1204–1207.

Chen, G., 2004. Electrochemical technologies in wastewater treatment. Sep. Purif. Technol. 38, 11–41.

Chideroli, R.T., Amoroso, N., Mainardi, R.M., Suphoronski, S.A., de Padua, S.B., Alfieri, A.F., Alfieri, A.A., Mosela, M., Moralez, A.T.P., de Oliveira, A.G., Zanolo, R., Di Santis, G.W., Pereira, U.P., 2017. Emergence of a new multidrug-resistant and highly virulent serotype of Streptococcus agalactiae in fish farms from Brazil. Aquaculture 479, 45–51.

Coledam, D.A.C., Aquino, J.M., Silva, B.F., Silva, A.J., Rocha-Filho, R.C., 2016. Electrochemical mineralization of norfloxacin using distinct boron-doped diamond anodes in a filter-press reactor, with investigations of toxicity and oxidation by-products. Electrochim. Acta 213, 856–864.

Comninellis, C., 1994. Electrocatalysis in the Electrochemical Conversion / Combustion of Organic Pollutants. Electrochim. Acta 39, 1857–1862.

Comninellis, C., Chen, G., 2010. Electrochemistry for the Environment, Electrochemistry for the Environment. Springer New York, New York, NY.

da Silva, A.J.C., dos Santos, E.V., de Oliveira Morais, C.C., Martínez-Huitle, C.A., Castro, S.S.L., 2013. Electrochemical treatment of fresh, brine and saline produced water generated by petrochemical industry using Ti/IrO2-Ta2O5 and BDD in flow reactor. Chem. Eng. J. 233, 47–55.

da Silva, S.W., Heberle, A.N.A., Santos, A.P., Rodrigues, M.A.S., Pérez-Herranz, V., Bernardes, A.M., 2018. Antibiotics mineralization by electrochemical and UV-based hybrid processes: evaluation of the synergistic effect. Environ. Technol. 1–11.

Daghrir, R., Drogui, P., Tshibangu, J., 2014. Efficient treatment of domestic wastewater by electrochemical oxidation process using bored doped diamond anode. Sep. Purif. Technol. 131, 79–83.

Davis, J., Baygents, J.C., Farrell, J., 2014. Understanding persulfate production at boron doped diamond film anodes. Electrochim. Acta 150, 68–74.

de Araújo, D.M., Cañizares, P., Martínez-Huitle, C.A., Rodrigo, M.A., 2014. Electrochemical conversion/combustion of a model organic pollutant on BDD anode: Role of sp3/sp2 ratio. Electrochem. commun. 47, 37–40.

de Moura, D.C., de Araújo, C.K.C., Zanta, C.L.P.S., Salazar, R., Martínez-Huitle, C.A., 2014. Active chlorine species electrogenerated on Ti/Ru0.3Ti0.7O2 surface: Electrochemical behavior, concentration determination and their application. J. Electroanal. Chem. 731, 145–152.

de Queiroz, J.L.A., da Silva, A.R.L., de Moura, D.C., da Silva, D.R., Martínez-Huitle, C.A., 2017. Electrochemical study of carboxylic acids with Nb-supported boron doped diamond anode. Part 1: Potentiodynamic measurements and bulk oxidations. J. Electroanal. Chem. 794, 204–211.

de Souza Santos, L.V., Meireles, A.M., Lange, L.C., 2015. Degradation of antibiotics norfloxacin by Fenton, UV and UV/H2O2. J. Environ. Manage. 154, 8–12.
Einaga, Y., Foord, J.S., Swain, G.M., 2014. Diamond electrodes: Diversity and maturity. MRS Bull. 39, 525–532.
Fierro, S., Abe, K., Christos, C., Einaga, Y., 2011. Influence of Doping Level on the Electrochemical Oxidation of Formic Acid on Boron Doped Diamond Electrodes. J. Electrochem. Soc. 158, F183–F189.
Fukunaga, M.T., Guimarães, J.R., Bertazzoli, R., 2008. Kinetics of the oxidation of formaldehyde in a flow electrochemical reactor with TiO2/RuO2 anode. Chem. Eng. J. 136, 236–241.
Galizzioli, D., Tantardini, F., Trasatti, S., 1974. Ruthenium dioxide: a new electrode material. I. Behaviour in acid solutions of inert electrolytes. J. Appl. Electrochem. 4, 57–67.
García-Galbadón, M., Pérez-Herranz, V., García-Antón, J., Guiñón, J.L., 2006. Electrochemical recovery of tin from the activating solutions of the electroless plating of polymers. Galvanostatic operation. Sep. Purif. Technol. 51, 143–149.
Garcia-Segura, S., Vieira dos Santos, E., Martínez-Huitle, C.A., 2015. Role of sp3/sp2 ratio on the electrocatalytic properties of boron-doped diamond electrodes: A mini review. Electrochem. commun. 59, 52–55.
Gargouri, B., Gargouri, O.D., Gargouri, B., Trabelsi, S.K., Abdelhedi, R., Bouaziz, M., 2014. Application of electrochemical technology for removing petroleum hydrocarbons from produced water using lead dioxide and boron-doped diamond electrodes. Chemosphere 117, 309–315.
González, O., Justo, A., Bacardit, J., Ferrero, E., Malfeito, J.J., Sans, C., 2013. Characterization and fate of effluent organic matter treated with UV/H2O2 and ozonation. Chem. Eng. J. 226, 402–408.
Guinea, E., Centellas, F., Brillas, E., Cañizares, P., Sáez, C., Rodrigo, M.A., 2009. Electrocatalytic properties of diamond in the oxidation of a persistant pollutant. Appl. Catal. B Environ. 89, 645–650.
Heberle, A.N.A., da Silva, S.W., Klauck, C.R., Ferreira, J.Z., Rodrigues, M.A.S., Bernardes, A.M., 2017. Electrochemical enhanced photocatalysis to the 2,4,6 Tribromophenol flame retardant degradation. J. Catal. 351, 136–145.
Isarain-Chávez, E., Baró, M.D., Rossinyol, E., Morales-Ortiz, U., Sort, J., Brillas, E., Pellicer, E., 2017. Comparative electrochemical oxidation of methyl orange azo dye using Ti/Ir-Pb, Ti/Ir-Sn, Ti/Ru-Pb, Ti/Pt-Pd and Ti/RuO 2 anodes. Electrochim. Acta 244, 199–208.
Kapałka, A., Fóti, G., Comninellis, C., 2008. Kinetic modelling of the electrochemical mineralization of organic pollutants for wastewater treatment. J. Appl. Electrochem. 38, 7–16.
Kümmerer, K., 2009. Antibiotics in the aquatic environment - A review - Part I. Chemosphere. 75, 417–434.
Leal, R.M.P., Alleoni, L.R.F., Tornisielo, V.L., Regitano, J.B., 2013. Sorption of fluoroquinolones and sulfonamides in 13 Brazilian soils. Chemosphere 92, 979–985.
Lin, H., Niu, J., Ding, S., Zhang, L., 2012. Electrochemical degradation of perfluorooctanoic acid (PFOA) by Ti/SnO 2-Sb, Ti/SnO 2-Sb/PbO 2 and Ti/SnO 2-Sb/MnO 2 anodes. Water Res. 46, 2281–2289.
Martin, H.B., Argoitia, A., Landau, U., Anderson, A.B., Angus, J.C., 1996. Hydrogen and Oxygen Evolution on Boron-Doped Diamond Electrodes. J. Electrochem. Soc. 143, L133–L136.
Miao, X.S., Bishay, F., Chen, M., Metcalfe, C.D., 2004. Occurrence of antimicrobials in the final effluents of wastewater treatment plants in Canada. Environ. Sci. Technol. 38, 3533–3541.
Panizza, M., Cerisola, G., 2009. Direct and mediated anodic oxidation of organic pollutants. Chem. Rev. 109, 6541–6569.
Pelegrini, R., Peralta-Zamora, P., De Andrade, A.R., Reyes, J., Durán, N., 1999. Electrochemically

assisted photocatalytic degradation of reactive dyes. Appl. Catal. B Environ. 22, 83–90.
Provent, C., Haenni, W., Santoli, E., Rychen, P., 2004. Boron-doped diamond electrodes and microelectrode-arrays for the measurement of sulfate and peroxodisulfate. Electrochim. Acta 49, 3737–3744.
Rice, E.W., Baird, R.B., Eaton, A.D., 2017. Standard Methods for the Examination of Water and Wastewater, in: Rice, E.W., Baird, R.B., Eaton, A.D. (Eds.), American Public Health Association. American Public Health Association, American Water Works Association, Water Environment Federation, p. 1504–1507.
Sales Solano, A.M., Costa de Araújo, C.K., Vieira de Melo, J., Peralta-Hernandez, J.M., Ribeiro da Silva, D., Martínez-Huitle, C.A., 2013. Decontamination of real textile industrial effluent by strong oxidant species electrogenerated on diamond electrode: Viability and disadvantages of this electrochemical technology. Appl. Catal. B Environ. 130–131, 112–120.
Serrano, K., Michaud, P.A., Comninellis, C., Savall, A., 2002. Electrochemical preparation of peroxodisulfuric acid using boron doped diamond thin film electrodes. Electrochim. Acta 48, 431–436.
Souza, F., Quijorna, S., Lanza, M.R. V, Saéz, C., Cañizares, P., Rodrigo, M.A., 2017. Applicability of electrochemical oxidation using diamond anodes to the treatment of a sulfonylurea herbicide. Catal. Today 280, 192–198.
Souza, F.L., Saéz, C., Lanza, M.R.V., Cañizares, P., Rodrigo, M.A., 2016. The effect of the sp3/sp2 carbon ratio on the electrochemical oxidation of 2,4-D with p-Si BDD anodes. Electrochim. Acta 187, 119–124.
Ternes, T.A., 1998. Occurrence of drugs in German sewage treatment plants and rivers. Water Res. 32, 3245–3260.
Thiele-Bruhn, S., 2003. Pharmaceutical antibiotic compounds in soils - A review. J. Plant Nutr. Soil Sci. 166, 145–167.
van den Bogaard, A.E., Stobberingh, E.E., 1999. Antibiotic Usage in Animals. Drugs 58, 589–607.
Watanabe, T., Shimizu, T.K., Tateyama, Y., Kim, Y., Kawai, M., Einaga, Y., 2010. Giant electric double-layer capacitance of heavily boron-doped diamond electrode. Diam. Relat. Mater. 19, 772–777.
Wenk, J., Von Gunten, U., Canonica, S., 2011. Effect of dissolved organic matter on the transformation of contaminants induced by excited triplet states and the hydroxyl radical. Environ. Sci. Technol. 45, 1334–1340.
Zhong, C., Wei, K., Han, W., Wang, L., Sun, X., Li, J., 2013. Electrochemical degradation of tricyclazole in aqueous solution using Ti/SnO2-Sb/PbO2 anode. J. Electroanal. Chem. 705, 68–74.

Figure Captions

Fig. 1 Electrodes characterization by cyclic voltammetry in 0.5 M H_2SO_4. **a** Influence of the boron concentration (Si/BDD_{100} × Si/BDD_{2500}); **b** Influence of the substrate of the diamond film (Si/BDD_{2500} × Nb/BDD_{2500}) and **c** Influence of material non-active (Nb/BDD_{2500}) × active (DSA®) for the OER.

Fig. 2 Cyclic voltammetry analysis for the electrochemical detection of oxidants electro-generated from supporting electrolyte in background solution containing 0.1 M Na_2SO_4. **a** Si/BDD_{100}; **b** Si/BDD_{2500}; **c** Nb/BDD_{2500} and **d** DSA®.

Fig. 3 Voltammetry response step-by-step adding NOR in background solution containing 0.1 M Na_2SO_4 for the electrodes. **a** Si/BDD_{100}; **b** Si/BDD_{2500}; **c** Nb/BDD_{2500} and **d** DSA®.

Fig. 4 Effect of boron concentration and diamond-sp^3/sp^2-carbon ratio on NOR oxidation. **a** Nor decay; **b** COD decay; **c** Current efficiency and **d** Energy consumption. Initial conditions: 30 L h^{-1}, 10 mA cm^{-2}, 0.1 mM NOR and 0.01 M Na_2SO_4.

Fig. 5 Effect of the diamond film substrate (Si or Nb) on NOR oxidation. **a** Nor decay; **b** COD decay; **c** Current efficiency and **d** Energy consumption. Initial conditions: 30 L h^{-1}, 10 mA cm^{-2}, 0.1 mM NOR and 0.01 M Na_2SO_4.

Fig. 6 Influence of the anode non-active (Nb/BDD_{2500}) and active (DSA®) for the oxygen evolution reaction (OER) for NOR oxidation. **a** Nor decay; **b** COD decay; **c** Current efficiency and **d** Energy consumption. Initial conditions: 30 L h^{-1}, 10 mA cm^{-2}, 0.1 mM NOR and 0.01 M Na_2SO_4.

Fig 7. The role of other components in real wastewater on the EAOP performance. **a** Experimental and theoretical NOR decay. Insert graphic is the linearized NOR decay profiles. **b** COD decay. NORE: real wastewater spiked with 0.1 mM NOR; NORES: real wastewater spiked with 0.1 mM NOR and 0.01 M Na_2SO_4; NOR: synthetic solution with 0.1 mM NOR and 0.01 M of Na_2SO_4. Initial conditions: 30 L h^{-1}, 10 mA cm^{-2} and Nb/BDD_{2500}.

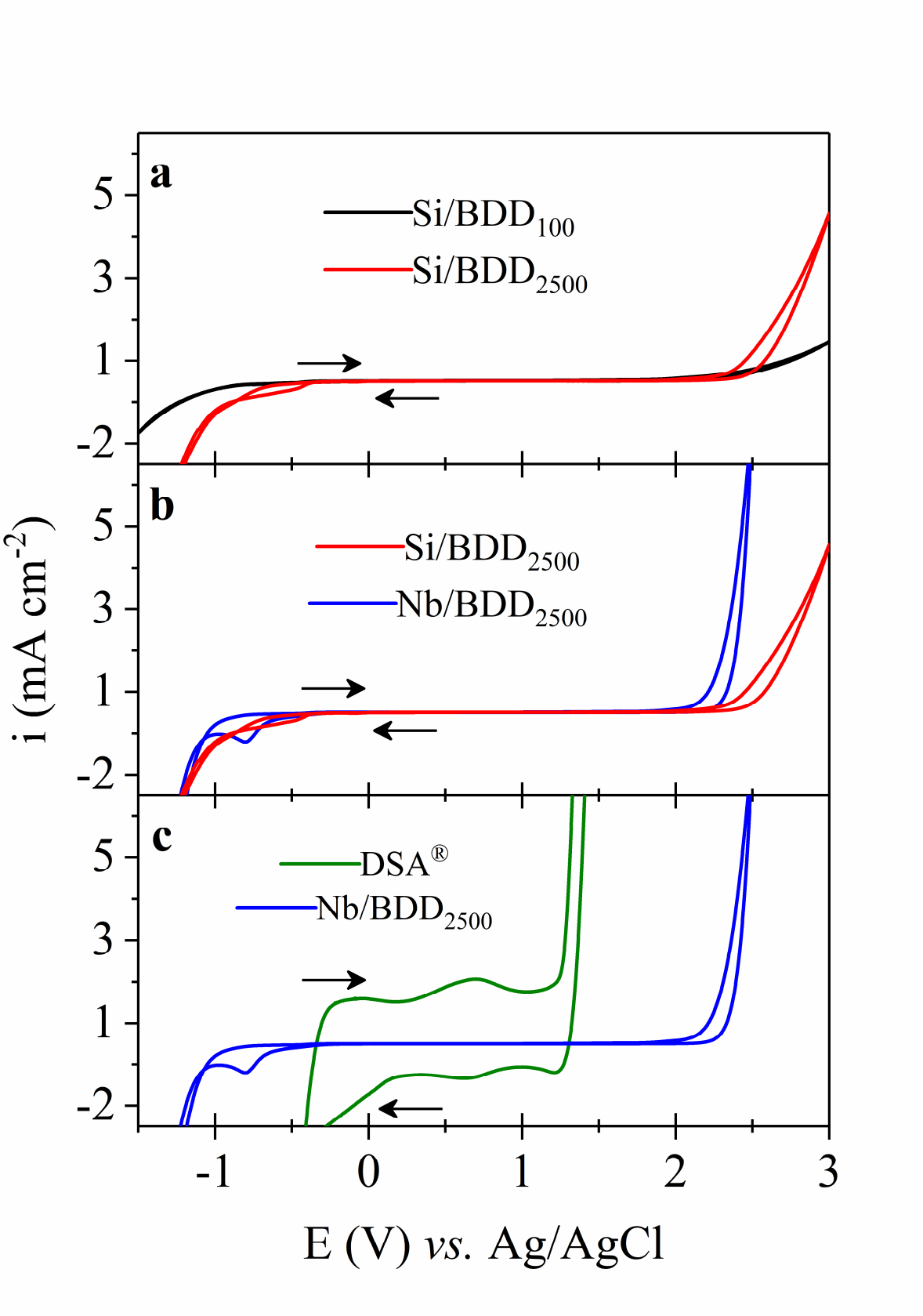
a
Si/BDD100
Si/BDD2500
b
Si/BDD2500
Nb/BDD2500
c
DSA®
Nb/BDD2500
i (mA cm-2)
E (V) vs. Ag/AgCl
5
3
1
-2
-1
0
1
2
3

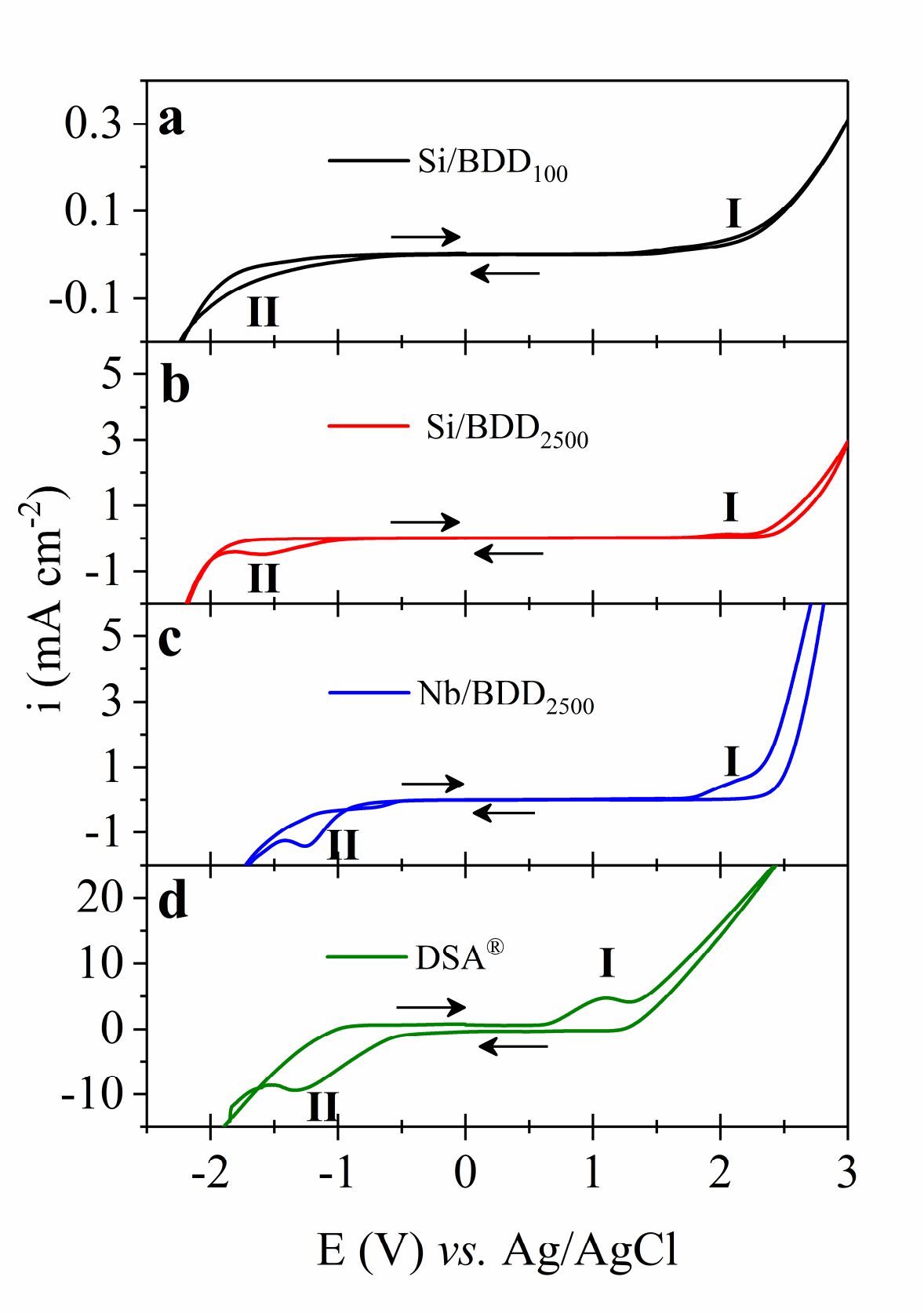
a
Si/BDD100
I
II
b
Si/BDD2500
I
II
c
Nb/BDD2500
I
II
d
DSA®
I
II
0.3
0.1
-0.1
5
3
1
-1
5
3
1
-1
20
10
0
-10
-2
-1
0
1
2
3
i (mA cm-2)
E (V) vs. Ag/AgCl

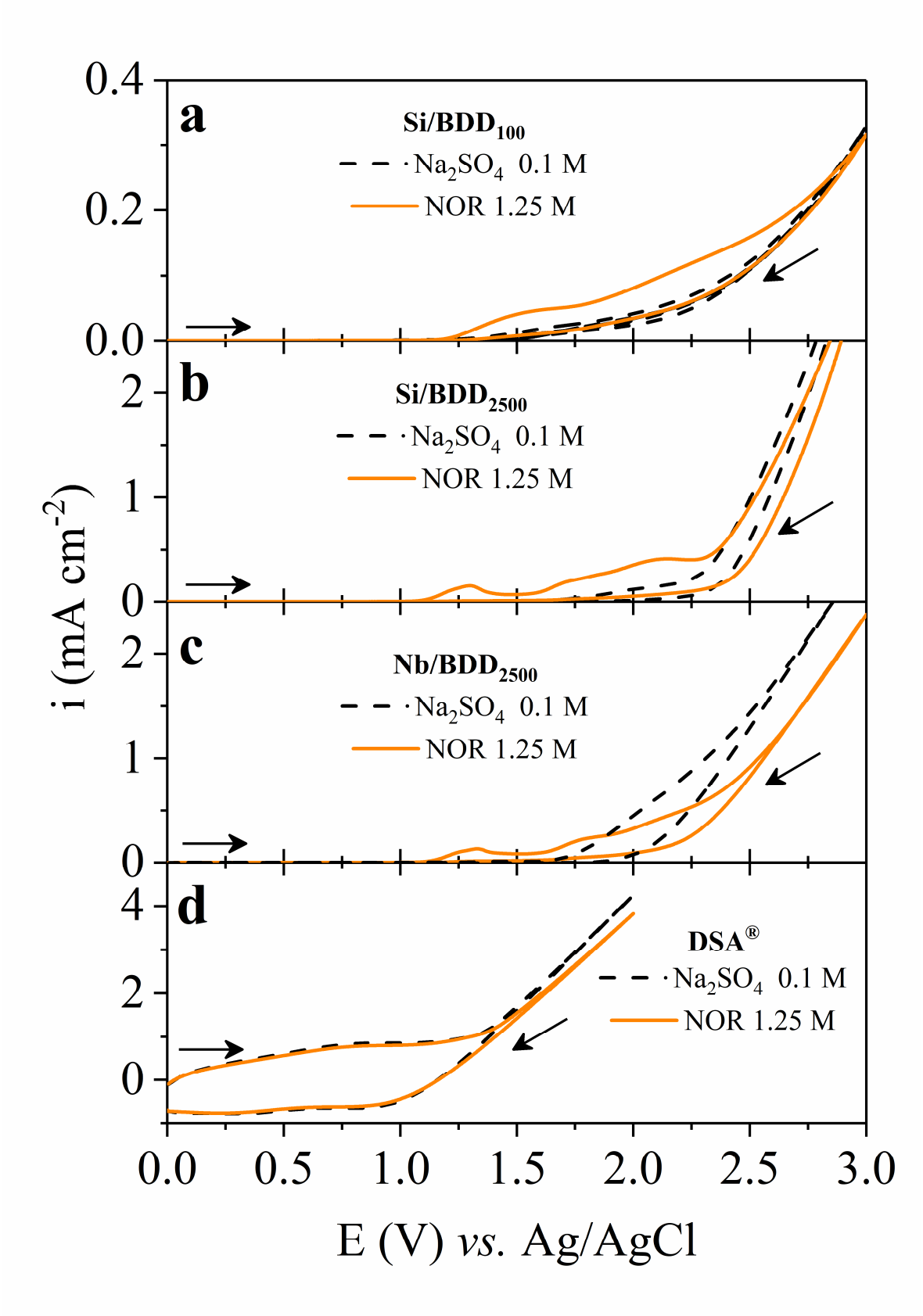
a
Si/BDD100
·Na2SO4 0.1 M
NOR 1.25 M
b
Si/BDD2500
·Na2SO4 0.1 M
NOR 1.25 M
c
Nb/BDD2500
·Na2SO4 0.1 M
NOR 1.25 M
d
DSA®
·Na2SO4 0.1 M
NOR 1.25 M
i (mA cm-2)
E (V) vs. Ag/AgCl

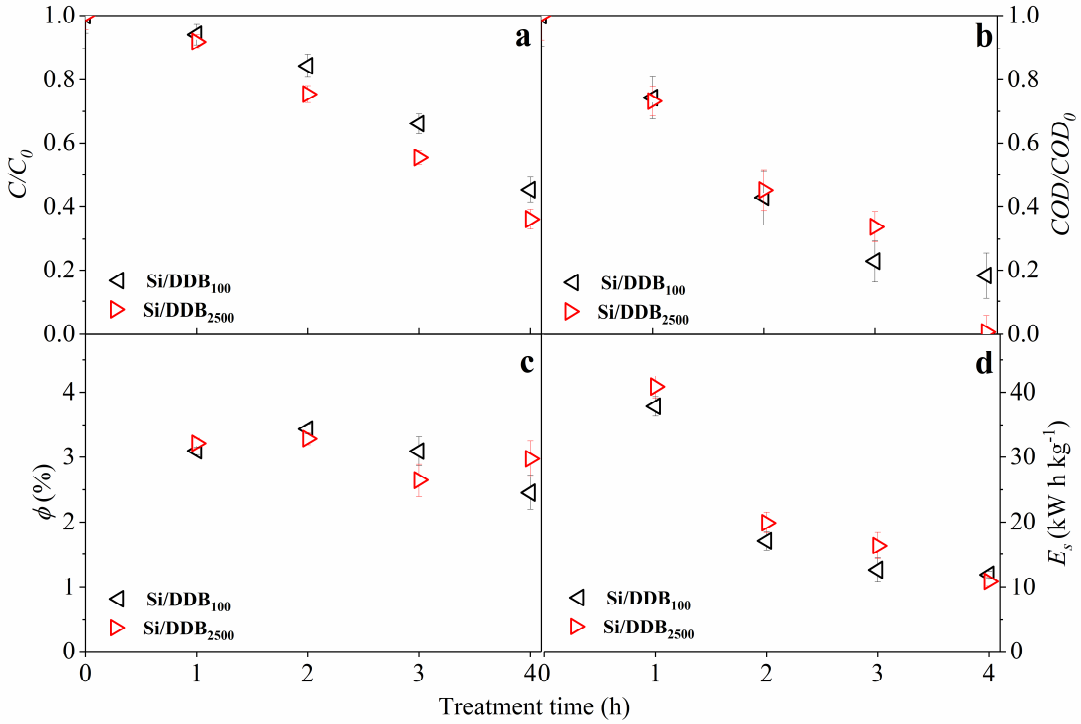

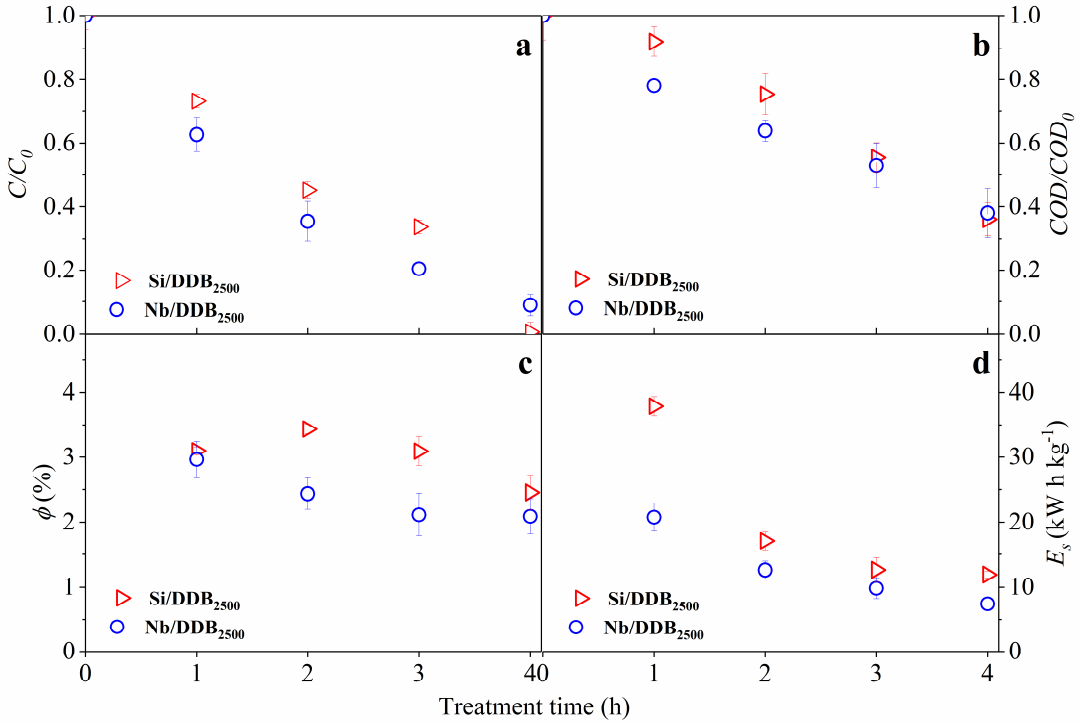

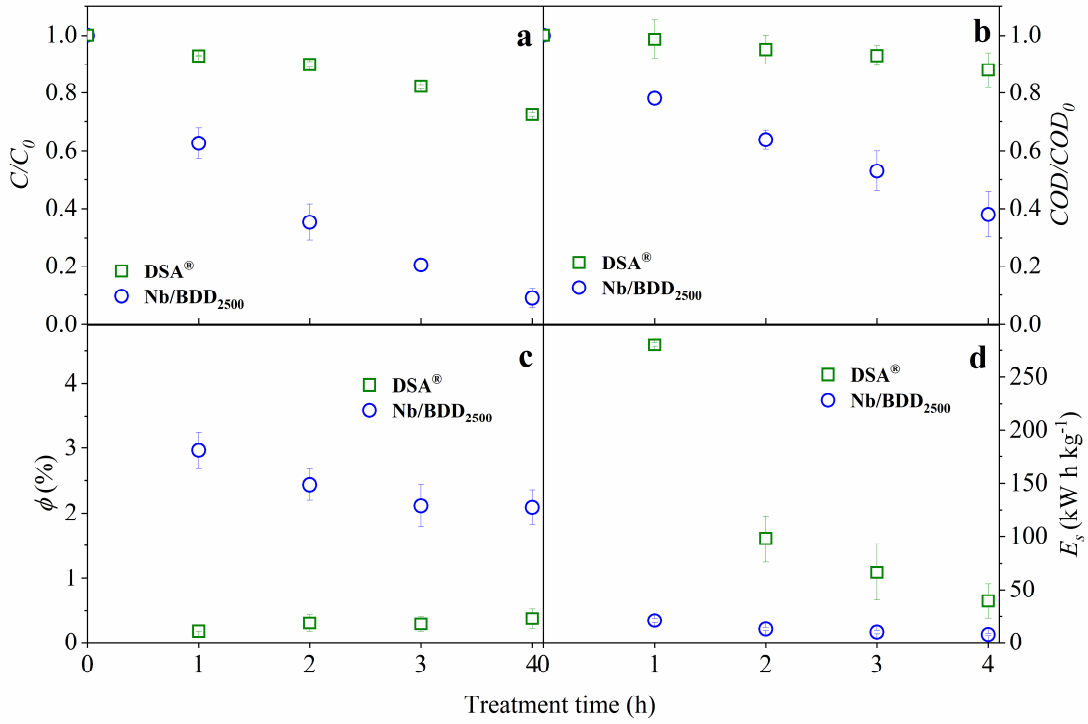

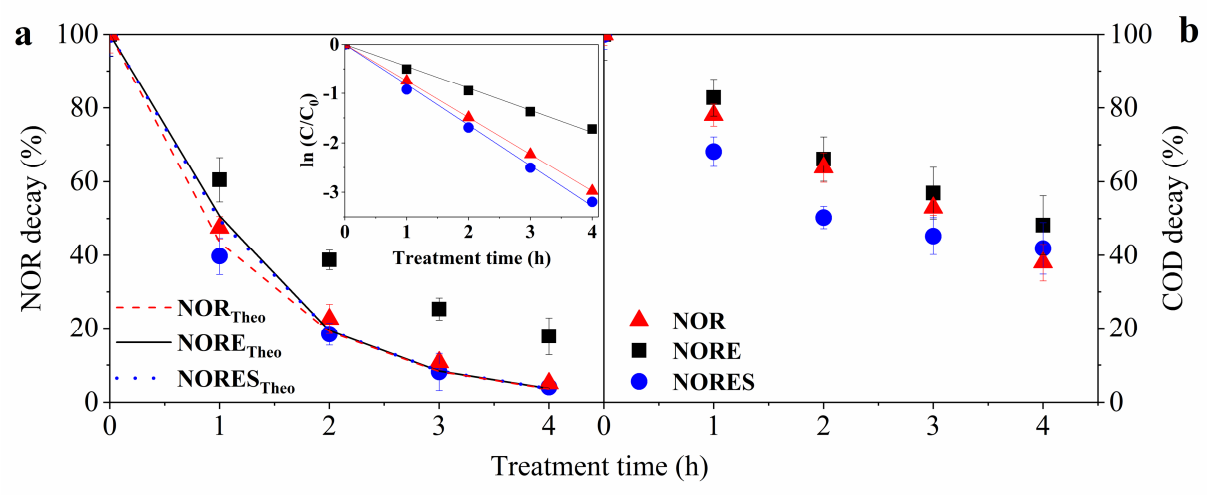

Highlights

- Electrochemical advanced Oxidation process is proposed for Norfloxacin oxidation
- Higher boron concentration favored NOR oxidation by persulfate and direct oxidation
- Persulfate and direct oxidation were more intense for the Nb/BDD than for Si/BDD
- Low difference in diamond-sp3/sp2-carbon ratio do not notably change NOR oxidation
- Nb/BDD showed similar current efficiency but lower energy consumption than Si/BDD